International Journal of Pharmaceutics 655 (2024) 124071

Contents lists available at ScienceDirect

International Journal of Pharmaceutics

journal homepage: www.elsevier.com/locate/ijpharm

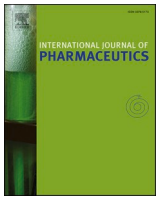

Parafilm® M and Strat-M® as skin simulants in *in vitro* permeation of dissolving microarray patches loaded with proteins

Qonita Kurnia Anjani [a,b], Avelia Devina Calista Nainggolan [c], Huanhuan Li [a], Andang Miatmoko [d,e], Eneko Larrañeta [a], Ryan F. Donnelly [a,*]

[a] School of Pharmacy, Queen's University Belfast, Medical Biology Centre, 97 Lisburn Road, Belfast BT9 7BL, UK
[b] Fakultas Farmasi, Universitas Megarezky, Jl. Antang Raya No. 43, Makassar 90234, Indonesia
[c] Faculty of Pharmacy, University of Indonesia, Depok 16424, Indonesia
[d] Faculty of Pharmacy, Airlangga University, Nanizar Zaman Joenoes Building, Campus C, Mulyorejo, Surabaya 60115, Indonesia
[e] Stem Cell Research and Development Center, Airlangga University, Institute of Tropical Disease Building, Campus C, Mulyorejo, Surabaya 60115, Indonesia

ARTICLE INFO

Keywords:
Parafilm® M
Strat-M®
Dermatomed porcine skin
Protein
Insertion studies
In vitro permeation studies

ABSTRACT

In vitro permeation studies play a crucial role in early formulation optimisation before extensive animal model investigations. Biological membranes are typically used in these studies to mimic human skin conditions accurately. However, when focusing on protein and peptide transdermal delivery, utilising biological membranes can complicate analysis and quantification processes. This study aims to explore Parafilm®M and Strat-M® as alternatives to dermatomed porcine skin for evaluating protein delivery from dissolving microarray patch (MAP) platforms. Initially, various MAPs loaded with different model proteins (ovalbumin, bovine serum albumin and amniotic mesenchymal stem cell metabolite products) were prepared. These dissolving MAPs underwent evaluation for insertion properties and *in vitro* permeation profiles when combined with different membranes, dermatomed porcine skin, Parafilm®M, and Strat-M®. Insertion profiles indicated that both Parafilm®M and Strat-M® showed comparable insertion depths to dermatomed porcine skin (in range of 360–430 μm), suggesting promise as membrane substitutes for insertion studies. In *in vitro* permeation studies, synthetic membranes such as Parafilm®M and Strat-M® demonstrated the ability to bypass protein-derived skin interference, providing more reliable results compared to dermatomed neonatal porcine skin. Consequently, these findings present valuable tools for preliminary screening across various MAP formulations, especially in the transdermal delivery of proteins and peptides.

1. Introduction

Protein and peptide-based therapies have gained prominence in treating various chronic diseases, often being the primary therapeutic choice (Kirkby et al., 2020; Bruno et al., 2013). Market estimates reveal a significant growth in the protein and peptide drug market, currently nearing US$40 billion annually, outpacing the small molecule market (Bruno et al., 2013). This steady growth underscores the ongoing investigation and advancements in protein and peptide delivery methods, catering especially to diseases once deemed incurable. While intravenous injection ensures 100% bioavailability, its preference diminishes for frequent administration in chronic diseases (Kirkby et al., 2020; Antosova et al., 2009; Jiskoot et al., 2012). Subcutaneous injection of antibodies and peptides has been employed, allowing for potential self-administration by patients at home (Doughty et al., 2016; Bittner et al., 2018). However, patients seek alternatives in the form of self-administrable, painless, and minimally invasive dosage forms to reduce hospital visits and alleviate the healthcare burden associated with therapy (Anjani et al., 2023a). Transdermal drug delivery, notably *via* microarray patches (MAPs), emerges as a potential solution. MAP technology, intensively researched in biomedicine, aims to facilitate effective drug and vaccine delivery (Donnelly and Prausnitz, 2023; Vora et al., 2023). MAPs function by painlessly breaching the *stratum corneum* (SC), creating microchannels to aid drug diffusion into deeper dermal layers (Anjani et al., 2022a). This approach circumvents passive drug diffusion challenges, allowing delivery of a wide range of chemical

* Corresponding author at: Chair in Pharmaceutical Technology, School of Pharmacy, Queen's University Belfast, Medical Biology Centre, 97 Lisburn Road, Belfast BT9 7BL, Northern Ireland, UK.
E-mail address: r.donnelly@qub.ac.uk (R.F. Donnelly).

https://doi.org/10.1016/j.ijpharm.2024.124071
Received 10 January 2024; Received in revised form 27 March 2024; Accepted 28 March 2024
Available online 29 March 2024

substances irrespective of molecular size and lipophilicity (Anjani et al., 2021b; Alkilani et al., 2015; Oberli et al., 2014). MAPs also offer advantages such as non-splanchnic absorption, avoidance of gastrointestinal degradation, and bypassing hepatic first-pass metabolism (Anjani et al., 2023b; Larrañeta et al., 2016). Consequently, the utilisation of MAPs holds significant promise in enhancing protein and peptide therapy.

In transdermal drug delivery, *in vitro* permeation studies play a pivotal role in assessing system suitability before extensive animal model investigations. Human or animal excised skin serves as the gold standard for such evaluations (Haq et al., 2018). However, their availability is constrained due to ethical considerations and limited sources. Additionally, these biological membranes entail complex preparation processes, have a short lifespan, and exhibit high variability (Haq et al., 2018; Neupane et al., 2020). Accordingly, excised skin cannot be used as a standardised material for pharmacopeial or quality control test. Furthermore, when focusing on protein and peptide transdermal delivery, using biological membranes in permeation studies complicates analysis and quantification processes. Particularly in quantification using microBCA protein assay kits, distinguishing between skin-sourced protein and that permeated from the MAP presents a challenge. Hence, there's a crucial need to identify substitutes for biological membranes suitable for this experimental design.

This study proposes, for the first time, the use of artificial membranes, Parafilm®M and Strat-M®, as skin simulants for *in vitro* permeation studies. Strat-M® membrane has been reported to be a promising alternative to biological membrane for the permeation of different chemical compounds in *in vitro* studies of transdermal patches (Haq et al., 2018; Pulsoni et al., 2022; Uchida et al., 2016). Moreover, Parafilm®M also has been studied and proposed to be a validated skin simulant for a rapid quality control of MAP in terms of evaluation of insertion profile (Larrañeta et al., 2014).

In the present study, we conducted a comparative study, assessing the permeation of three model proteins (ovalbumin (OVA) and bovine serum albumin (BSA) and amniotic mesenchymal stem cell metabolite products (AMSC-MP)) through these membranes and dermatomed neonatal porcine skin. Additionally, we evaluated and compared the insertion profile of dissolving MAPs containing peptides or proteins with *ex vivo* dermatomed porcine skin. To the best of our knowledge, there is only one published study that focuses on the use of artificial membranes tailored specifically for MAP applications in *in vitro* studies (Garland et al., 2012). Garland *et al.* explored the utilisation of Silescol® as a skin simulant in *in vitro* studies for small molecules. Their findings indicated a comparatively lower cumulative percentage permeation of model compounds across the Silescol® membrane when compared to neonatal porcine skin, which is not ideal for such applications. Therefore, this work would greatly benefit researchers to with limited access to animal skin tissue and lacking specialised mass spectrophotometers for quantifying protein and peptide-based drug permeation from MAP platforms.

2. Materials and methods

2.1. Materials

Albumin (chicken egg, ovalbumin) and bovine serum albumin (BSA) (lyophilised powder), poly(vinyl alcohol) (PVA) (MW 9–10 kDa, 80% hydrolysed) and poly(vinyl pyrrolidone) (PVP) K90 (MW 360 kDa) were purchased from Sigma-Aldrich (Dorset, UK). Amniotic mesenchymal stem cell metabolite products (AMSC-MP) lyophilised powder was obtained from the Stem Cell Research and Development Center, Airlangga University, Indonesia. Poly (vinyl pyrrolidone) (PVP) K29/32 (MW 58 kDa) were provided by Ashland (Kidderminster, UK). Strat-M® transdermal diffusion test model was purchased from Merck (Darmstadt, Germany). Parafilm® M was purchased from Amcor (Zürich, Switzerland). All other chemicals and materials were of analytical grade and purchased from Sigma-Aldrich (Dorset, UK) or Fisher Scientific (Loughborough, UK). Neonatal porcine skin was obtained from stillborn piglets less than 24 h after birth, rinsed in phosphate buffer saline (PBS pH 7.4), dermatomed to a thickness of 350 μm, and kept frozen at −20°C until use.

2.2. Preparation of dissolving MAPs

An aqueous blend containing 40% w/v PVA and 40% w/v PVP K29/32 with ratio 1:1, called PP2 (Anjani et al., 2023c), was used to prepare dissolving MAPs, as outlined in Table 1. A 50 mg aliquot of each formulation was poured into silicone mould (0.5 cm^2 needle area, 16 × 16 pyramidal-cuboidal holes, 850 μm needle height and 300 μm width at the base, illustrated in Fig. 1) placed into pressure chamber for 5 mins at 5 bar. Furthermore, the moulds were removed from pressure chamber and the excess of formulation was removed from the mould surface, and then centrifuged at 5000 rpm for 10 mins with the temperature controlled at 4°C. Following this, a silicone ring (internal diameter 18 mm and thickness 3 mm) was glued on to the mould surface using 40% w/v PVA aqueous solution and dried at ambient temperature for 24 h. The second layer of dissolving MAP was prepared by poured 500 μg of aqueous solution of 30% w/v PVP K90 and 1.5% glycerol, centrifuged at 5000 rpm for 10 mins at 4°C, allowed to dry under ambient conditions for 24 h. Sidewalls of dissolving MAPs were removed using scissors and then transferred into oven 37°C for final drying for 24 h.

2.3. Optical coherence tomography and pore visualisation

Each dissolving MAP was inserted into a membrane models (dermatomed skin, Parafilm and Strat-M) using a TA-TX2 Texture Analyser (TA) (Stable Microsystems, Haslemere, UK), as previously described (Bin Sabri et al., 2021; Bin Sabri et al., 2022; Anjani et al., 2022b) and illustrated in Fig. 2, with a 32 N force was applied, which equal to force released by human thumb pressure (Larrañeta et al., 2014). A piece of dental wax was applied under the membrane to protect the tips of the needles piercing the membrane (Bin Sabri et al., 2021; Bin Sabri et al., 2022; Anjani et al., 2022b). The insertion and holes were observed and visualised using EX-101 optical coherence tomography (OCT) microscope (Michelson Diagnostics Ltd., Kent, UK), digital light microscope (Leica EZ4 D, Leica Microsystems, Milton Keynes, UK) and scanning electron microscope (SEM) TM3030 microscope (Hitachi, Krefeld, Germany). The images obtained from OCT analysis was then processed and analysed using ImageJ® (National Institutes of Health, Bethesda MD, USA).

2.4. Determination of protein released from membranes

To anticipate any proteins that might interfere with the quantification of proteins sourced from membranes (including dermatomed neonatal porcine skin, Strat-M®, and Parafilm®) during the *in vitro* studies in the Franz cell setup, a release study was conducted as a preliminary step before the *in vitro* permeation studies. Each membrane was trimmed into a circular shape measuring 1.5 cm^2, equivalent to the area of inner part of the donor compartment in the Franz cell apparatus. These membranes were then placed into separate vials containing 12 mL of PBS (pH 7.4) and incubated in a shaker incubator (Jeio Tech ISF-7100, Medline Scientific, Chalgrove Oxon, UK) at 37°C for 24 h. Subsequently, the samples were analysed using a micro-BCA kit, and if

Table 1
Formulation of first layer dissolving MAP.

Composition	Protein Type		AMSC-MP
	Albumin	BSA	
Protein (%w/w)	10	10	10
Aqueous mixture PP2 (%w/w)	30	30	30
Deionised water (%w/w)	60	60	60

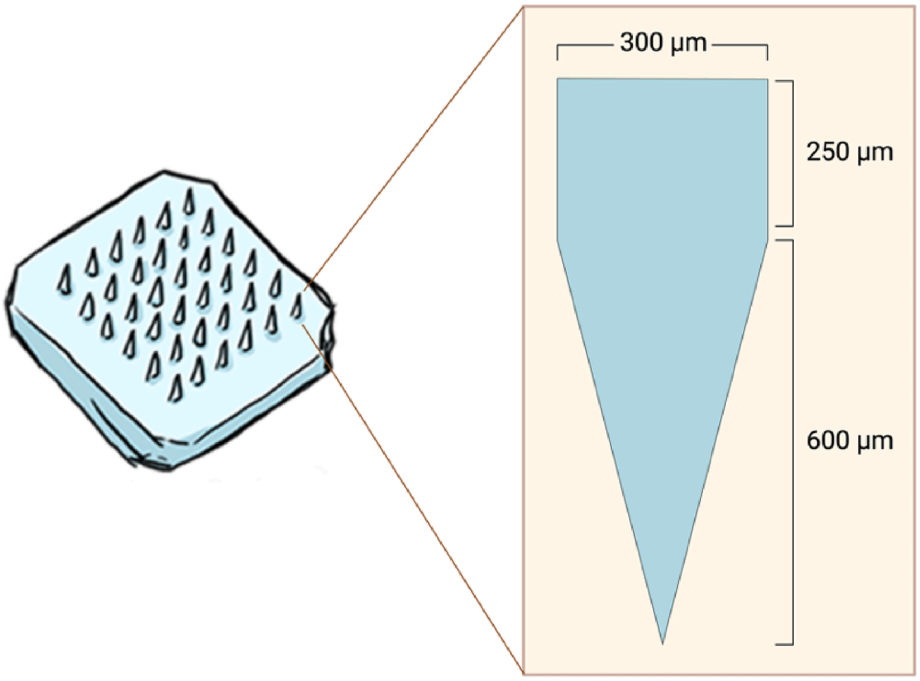

Fig. 1. Illustration of needle size and geometry on the array of dissolving MAP.

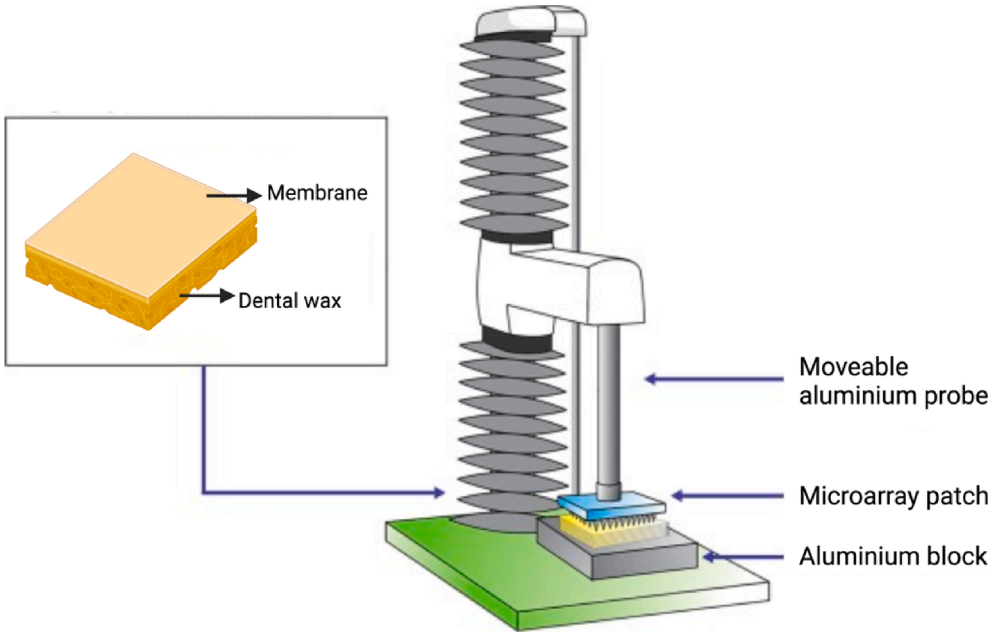

Fig. 2. Schematic illustration of texture analyser setup to evaluate dissolving MAP insertion properties into different membranes (dermatomed porcine skin, Strat-M® and Parafilm®).

necessary, the samples were diluted in PBS (pH 7.4).

2.5. *In vitro permeation studies using Franz cells*

For the *in vitro* permeation study, a Franz cell (Permergear, Hellertown PA, USA) setup was used with dermatomed neonatal porcine skin, Strat-M® and Parafilm®, as illustrated in Fig. 3. The porcine skin, obtained from stillborn piglets within 24 h post-mortem, was rinsed in PBS, dermatomed at the thickness of 350–400 µm, and frozen at −20°C until use. The membrane (dermatomed neonatal porcine skin, Strat-M® or Parafilm®) was carefully attached to the donor compartment of the Franz cell using cyanoacrylate glue. Preheated and degassed PBS (pH 7.4) was added to the receiver compartment, which was maintained at 37 ± 1°C and stirred at 600 rpm. The dissolving MAPs were manually pressed onto the skin for 30 s with a piece of dental wax underneath as described previously (Larrañeta et al., 2016). The drug-containing reservoir was placed on top of the dissolving MAPs, and the donor compartment was attached to the receiver compartment. A stainless-steel cylindrical weight (15.0 g) was placed on top of the reservoir to prevent MAP expulsion. The sampling arm of the receiver compartment and the donor compartment were sealed with Parafilm® M to prevent evaporation. At predetermined time points, 200 µL of release media was

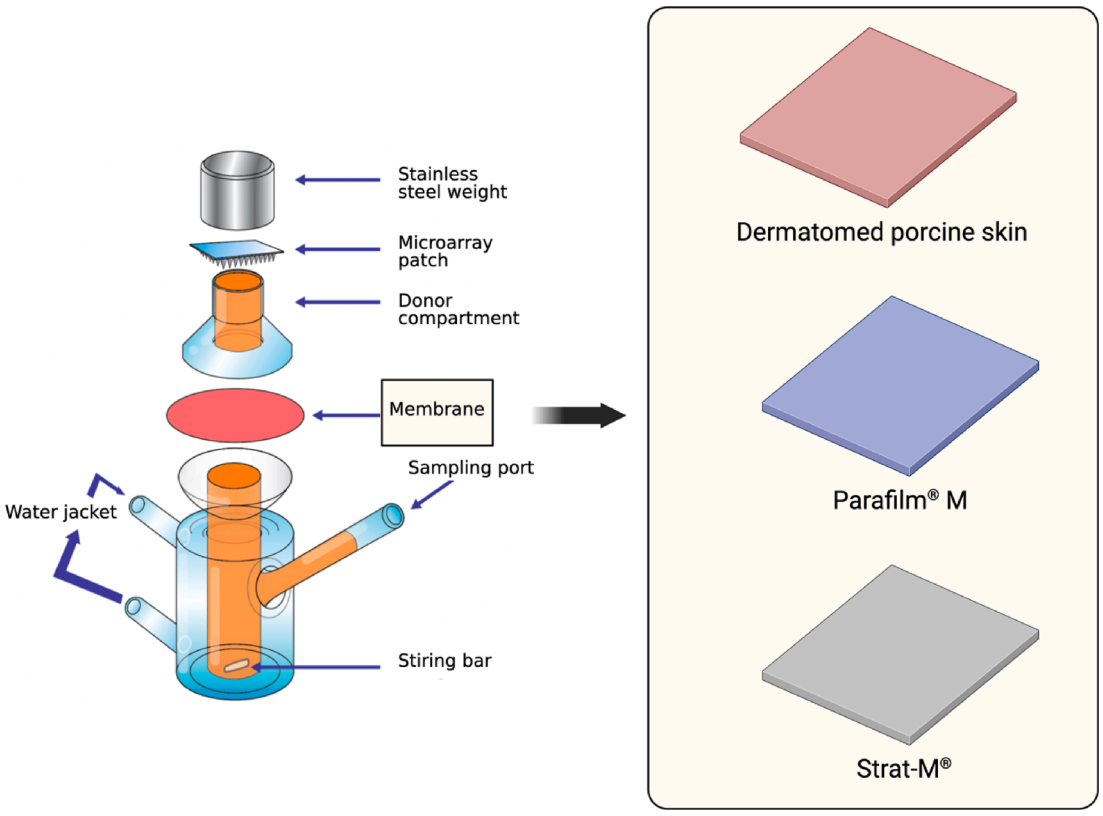

Fig. 3. Schematic illustration of Franz diffusion cell setup to assess permeation protein from dissolving MAP across different membranes (dermatomed porcine skin, Strat-M® and Parafilm®).

taken from the receiver compartment and analysed using micro-BCA kit. If necessary, samples were diluted in PBS (pH 7.4).

2.6. Quantification using micro-BCA protein assay kit

Samples from *in vitro* studies were quantified and analysing using Micro BCA™ Protein Assay Kit (Thermo Scientific, Rockford, IL, USA). Analysis was performed following the guideline provided by manufacturer. All samples were determined using a FluoStar Omega microplate reader (BMG Labtech, Germany) with spectroscopy principal with absorbance wavelength at 562 nm.

2.7. Statistical analysis

Statistical analysis was conducted using GraphPad Prism® version 8.0 (GraphPad Software, San Diego, California, USA). The experimental results were presented as means ± standard deviation (SD), unless otherwise specified. An unpaired *t*-test was used for comparing two cohorts, while one-way analysis of variance (ANOVA) was employed for comparing multiple cohorts.

3. Results and discussion

3.1. Preparation of dissolving MAPs

The study employed three distinct proteins as model substances (albumin derived from chicken eggs (OVA, MW 45 kDa), and bovine serum albumin (BSA, MW 66.5 kDa) and amniotic mesenchymal stem cell metabolite products (AMSC-MP, MW 76 kDa)). Dissolving MAPs containing these proteins were fabricated using the double casting method, as detailed in previous works (Anjani et al., 2022b; Anjani et al., 2022c; Anjani et al., 2022d). Moreover, proteins can be loaded into dissolving MAPs using more complex approaches such as coating the arrays with formulations containing proteins (Angkawinitwong et al., 2020; Caudill et al., 2018). In this study, each protein was loaded into the needle tips in a simple way and ensuring minimum waste of the protein cargo. For this purpose, the protein was combined with a mixture of PVA and PVP. Fig. 4 displays microscopic images of the resulting dissolving MAPs, demonstrating their homogeneity and well-defined structure, characterised by sharp needles. The needle shape is a combination of cuboidal and pyramidal, a result of the polydimethylsiloxane moulds used in this experiment. This mould design was chosen for its ability to facilitate effective insertion and drug delivery into the skin, which has shown superiority compared to other shapes (Cordeiro et al., 2020). Finally, these dissolving MAPs underwent subsequent insertion testing and *in vitro* permeation profiling.

3.2. Optical coherence tomography and pore visualisation

To assess the insertion capacity of protein-loaded MAPs into different membranes, dermatomed porcine skin (350–400 μm), Strat-M® (300 μm), and Parafilm®M (130 μm), the structures of which are illustrated in Fig. 5, specific membrane types were chosen for evaluation. The porcine skin utilised in this study was sourced from stillborn piglets and dermatomed to a thickness of 350 μm, comprising the epidermis (*stratum corneum, stratum granulosum, stratum spinosum*, and *stratum basal*) and the upper part of the dermis layer. This thickness was chosen because it approximates the distance from the skin surface to the dermal microcirculation. With a needle height of 850 μm, a proportion of the microneedles will be in direct contact with the receiver medium when using epidermal or upper dermal representations of the skin barrier (Garland et al., 2012). Strat-M®, engineered to mimic human skin structure, features a lipid-coated surface to simulate the *stratum corneum* layer (Haq et al., 2018). Below this lipid coating, Strat-M® consists of polyether sulfone, creating a more porous layer to mimic the dermis, followed by a polyolefin non-fabric support resembling the

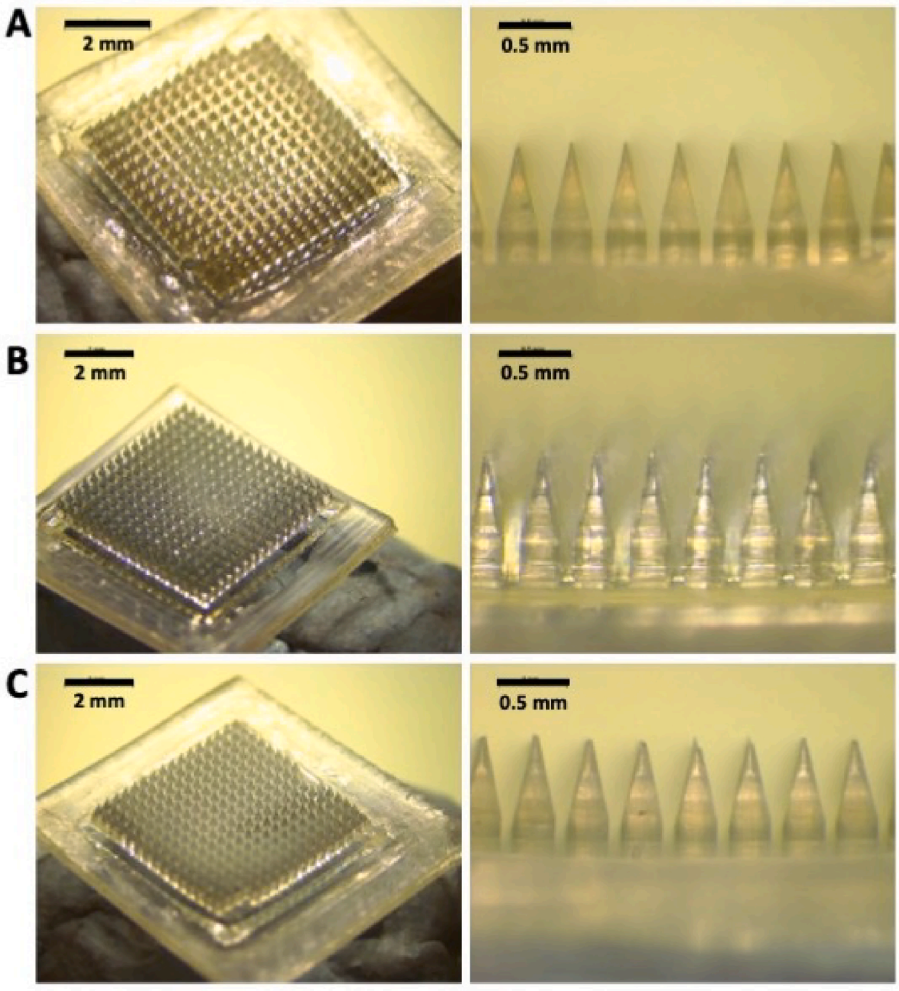

Fig. 4. Microscopic images of dissolving MAPs loaded with (A) albumin derived from chicken eggs (OVA), (B) bovine serum albumin (BSA), and (C) amniotic mesenchymal stem cell metabolite products (AMSC-MP).

subcutaneous layer (Haq et al., 2018; Pulsoni et al., 2022). Parafilm® was selected as a model membrane for this study due to its validation as a proposed membrane for MAP insertion studies (Larrañeta et al., 2014), serving as a rapid quality control test. Composed of a blend of hydrocarbon wax and polyolefin, Parafilm® replicates properties similar to the third layer of Strat-M®, aimed at simulating the subcutaneous layer. Although less structurally complex than actual skin and Strat-M®, Parafilm® provides sufficient hydrophobic properties, resembling the *stratum corneum*, which is a crucial barrier for MAP application.

OCT images in Fig. 6A–C illustrate the insertion of dissolving MAPs into various membranes. A clear gap is evident between the MAP baseplate and the membrane surfaces, suggesting incomplete penetration of dissolving MAPs into these membranes. As depicted in Fig. 6D–F, the microneedles of MAPs penetrated to depths of approximately 430 μm, 360 μm, and 400 μm for dermatomed porcine skin, Strat-M®, and Parafilm®, respectively. The insertion depth into dermatomed porcine skin aligns with previously published findings (Garland et al., 2012; Donnelly et al., 2010; Donnelly et al., 2011), significantly surpassing penetration depths observed in other skin simulants ($p < 0.05$). This disparity may be attributed to differences in membrane materials and elasticity compared to dermatomed porcine skin.

Notably, prior to the experiment, the porcine skin was equilibrated with PBS pH (7.4) to maintain skin integrity. The presence of saline water likely acted as a lubricant (Anjani et al., 2023d), facilitating deeper needle insertion compared to Strat-M® and Parafilm®. Furthermore, Parafilm® exhibited a deeper penetration compared to Strat-M®, possibly due to its single-layer thickness (~130 μm) versus the multilayered structure of Strat-M® (~300 μm). Fig. 7 confirms successful hole creation in all membranes, simulating piercing of the *stratum corneum* layer. However, while Strat-M® closely resembles the thickness of dermatomed porcine skin, detecting the holes in its deeper layers was challenging due to the polyolefin non-woven fabric's characteristics, mimicking the hypodermal layer and offering resistance to microneedle penetration. Despite the 10% and 16% differences in insertion depth between Parafilm® and Strat-M® compared to dermatomed porcine skin, both skin simulants show promise as membrane substitutes for insertion studies.

3.3. Determination of protein released from membranes

To assess protein release from various membranes, a preliminary study was conducted. Fig. 8 demonstrates that after incubating dermatomed neonatal porcine skin at 37°C for 24 h, approximately 39 mg of protein was released. Conversely, no protein was detected in either the Parafilm®M or Strat-M® groups. This outcome suggests that using biological membranes, coupled with the micro-BCA quantification method for protein delivery assessment, might yield unreliable results due to skin-derived proteins interfering with the delivered substance. Moreover, accounting for protein release from the blank dermatomed skin, we included the dermatomed porcine skin without dissolving MAP application in further *in vitro* permeation studies using the Franz cell setup. However, for both Parafilm®M and Strat-M®, no control or blank

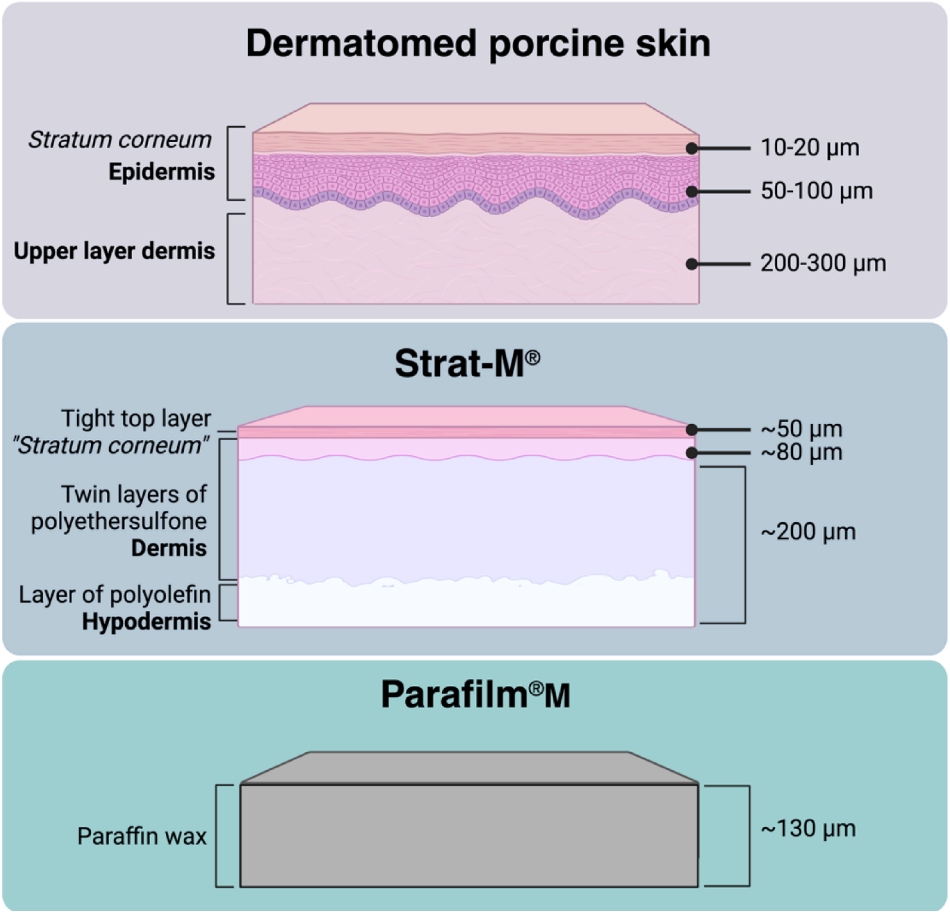

Fig. 5. Schematic illustration depicting the multilayer structure of dermatomed porcine skin alongside Strat-M® and a single layer of Parafilm®M.

groups were included as no protein was detected in this current study. This exclusion ensures the absence of protein interference during the quantification process in these cases.

3.4. *In vitro permeation studies using Franz cells*

The Franz cell setup was utilised in this study to evaluate the permeation of the protein models in an *in vitro* setting. This setup has consistently proven to be ideal in all our MAP-related studies for assessing the diffusion of molecules from the tip layer of MAPs to the skin layer, particularly across the epidermis-dermis boundary (Anjani et al., 2022a; Anjani et al., 2021b; Anjani et al., 2023; Bin Sabri et al., 2022; Anjani et al., 2022b; Anjani et al., 2022c; Anjani et al., 2022d; Anjani et al., 2021a; Anjani et al., 2023e; Anjani et al., 2023f). Conversely, *in vitro* release studies are not suitable for evaluating this process, as the entire patch is exposed to fluid media, leading to an overestimation of the drug release profile achieved from the dissolving MAP system. Therefore, we suggest using both membranes, Parafilm®M, and Strat-M®, as alternatives to biological membranes to assess the delivery of proteins and peptides in *in vitro* permeation studies using the Franz cell setup.

Fig. 9 displays the permeation profiles of model proteins released from polymeric dissolving MAPs across different membranes, dermatomed porcine skin, Parafilm®M, and Strat-M®. Both OVA and BSA permeation from dissolving MAPs demonstrated an initial rise within 2 h, followed by a plateau between 4 and 24 h for both Parafilm®M and Strat-M® membranes. In the case of AMSC-MP, notable differences were observed between Parafilm®M and Strat-M®. Across Parafilm®M, the protein permeation gradually increased from the first hour up to 6 h, increasing significantly at 24 h ($p < 0.05$). However, using Strat-M®, AMSC-MP permeated immediately within the first hour, maintaining a sustained permeation throughout the experimental period. The difference between the two membranes can be explained due to the effect of several factors. Strat-M® membrane is designed to mimic the skin and as can be seen in Fig. 7 dissolving MAPs do not go through the entire membrane. Therefore, proteins need to diffuse through the membrane as they are not directly in contact with the fluid of the receiver compartment. Dissolving MAPs can go through one layer of Parafilm® M (Fig. 7) and when placed in the receiver compartment, microneedles will be directly in contact with the fluid of the receiver compartment. That explains why permeation from Parafilm® M is faster.

The most substantial protein permeation facilitated by dissolving MAPs occurred when using dermatomed neonatal porcine skin as the model membrane. Burst release commenced within the first hour, followed by a marked sustained increase in cumulative permeation throughout the 24-hour experimental period. There is a possibility that dissolving MAPs penetrated through the dermatomed porcine skin, potentially expediting the rapid release into the receiver compartment. To assess the release of total protein content from dermatomed porcine skin without dissolving MAP application, we conducted an additional evaluation. Fig. 9 indicates a noticeable amount of protein release from the skin, even surpassing the total protein detected from both Parafilm®M and Strat-M® groups in all cases. This observation highlights that utilising any biological membrane can lead to false-positive results in protein permeation, as skin-derived proteins were detected and accumulated during the quantification process using the BCA method. Hence, employing synthetic membranes might alleviate this limitation associated with the quantification method.

Several studies have explored the delivery of BSA and OVA using the MAP platform. Badhe *et al.* developed chitosan-based MAPs coated with

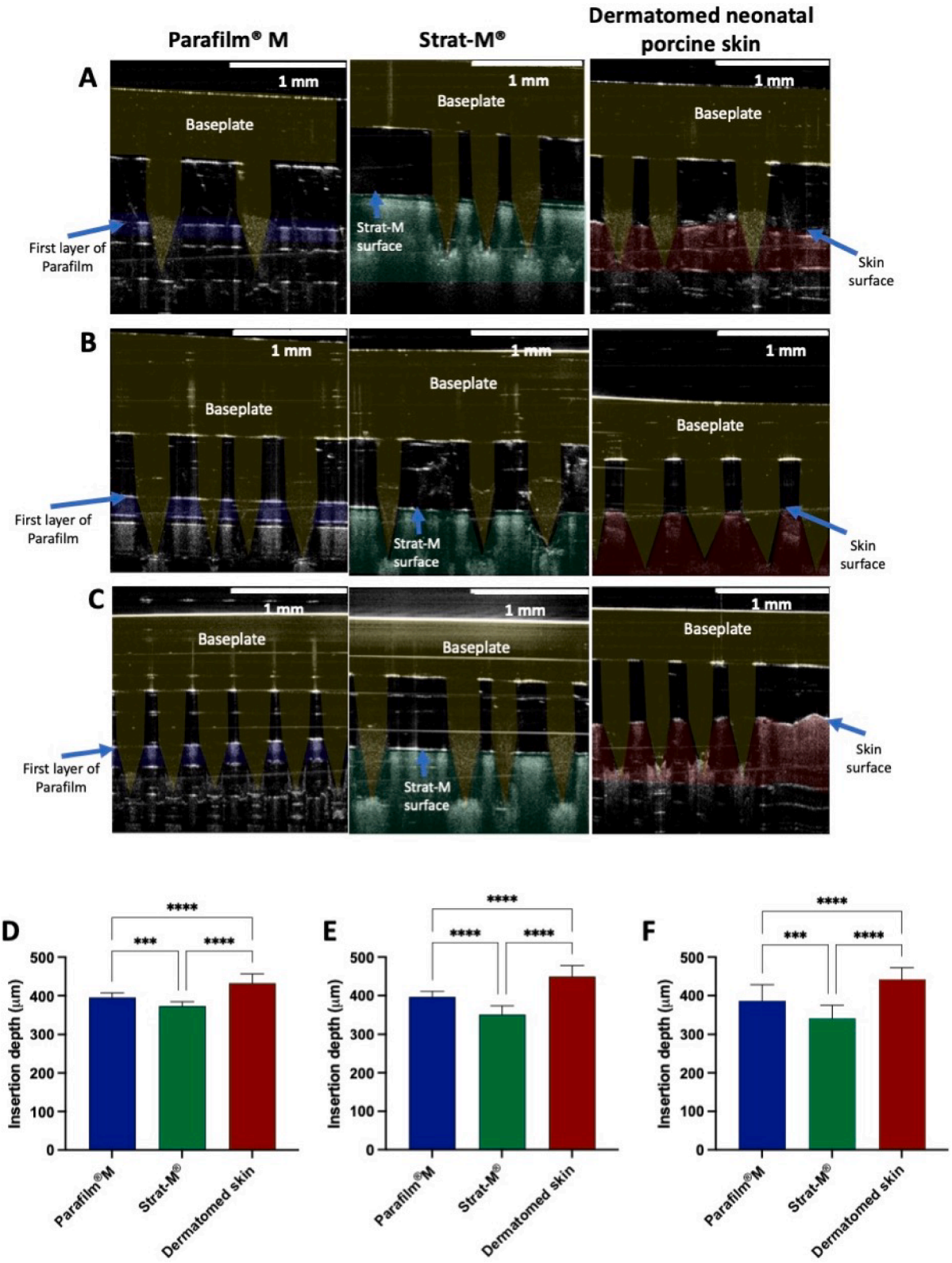

Fig. 6. OCT images of MAPs loaded with (A) albumin derived from chicken eggs (OVA), (B) bovine serum albumin (BSA), and (C) amniotic mesenchymal stem cell metabolite products (AMSC-MP) inserted into Parafilm®M, Strat-M® and dermatomed neonatal porcine skin following the application of pressure of 32 N for 30 s. The insertion depth of dissolving MAPs loaded with (D) albumin derived from chicken eggs (OVA), (E) bovine serum albumin (BSA), and (F) amniotic mesenchymal stem cell metabolite products (AMSC-MP) into Parafilm®M, Strat-M® and dermatomed neonatal porcine skin (means + SD, n = 20). To allow differentiation between dissolving MAP and the skin models, false colours were applied in the needles and skin model layers.

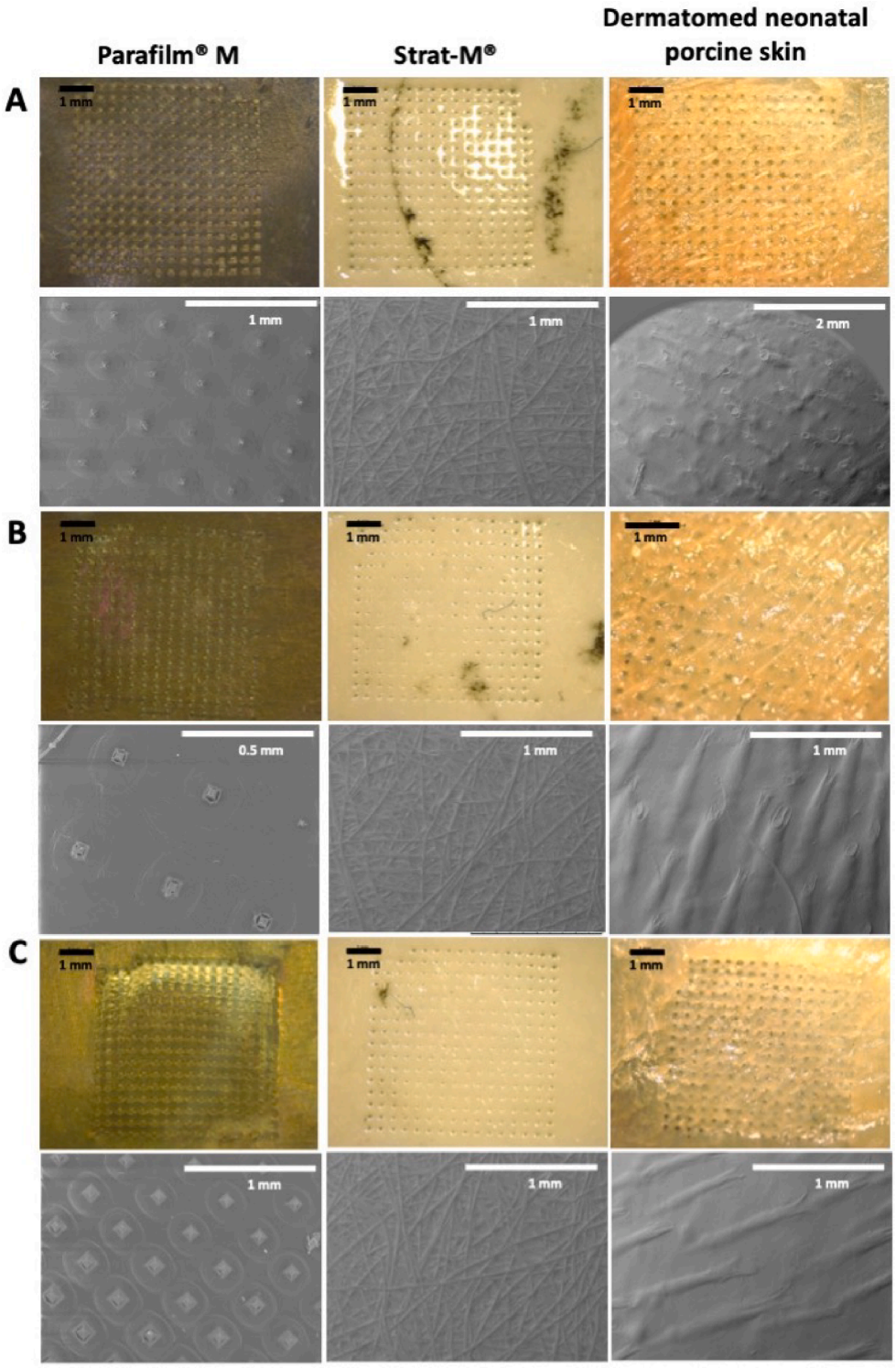

Fig. 7. Microscopic images of the upper layer and SEM images of the back side of each membrane were taken after the application of dissolving MAPs loaded with (A) albumin derived from chicken eggs (OVA), (B) bovine serum albumin (BSA), and (C) amniotic mesenchymal stem cell metabolite products (AMSC-MP) using a texture analyser with a 32 N pressure for 30 s.

BSA and poly(lactic acid) (Badhe et al., 2021). Using a colorimetric method with biuret reagent and a UV–Vis spectrophotometer set at a wavelength of 540 nm, the researchers quantified BSA release during an *in vitro* permeation study using Franz cells. The study revealed 98.5% BSA permeation across excised rat skin within 50 h (Badhe et al., 2021). However, it lacked a control group without MAP application, raising concerns about protein release from the skin during the study period.

Demir *et al.* developed sodium alginate-based MAPs loaded with BSA, indicating a higher percentage of BSA delivery (~14%) across dermatomed human abdominal skin compared to a transdermal patch (~1%) (Demir et al., 2013). The researchers quantified BSA release using the BCA method at 562 nm (Demir et al., 2013). Nevertheless, a control group analysis was missing, limiting understanding regarding the source of protein during these studies.

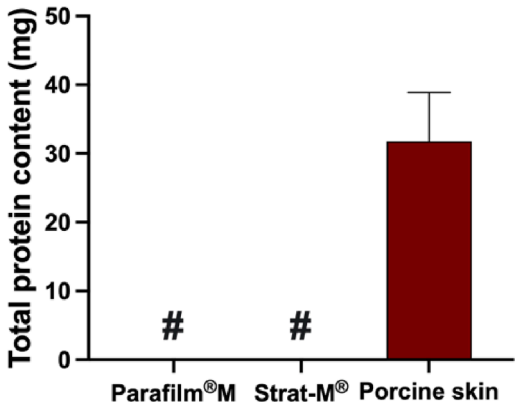

Fig. 8. The total protein released from each membrane after 24 h of incubation at 37°C in PBS (pH 7.4). The '#' symbol indicates that no protein was detected in the media (means + SD, n = 4).

Regarding OVA-mediated MAP permeation studies, Maaden *et al.* and Vallhov *et al.* utilised radiolabelled OVA (Van Der Maaden et al., 2014) and OVA conjugated with Alexa 488 (Vallhov et al., 2018), respectively. Maaden *et al.* employed a pH-sensitive MAP coated with radioactively labelled OVA and used an automatic gamma counter for specific quantification during *in vitro* permeation studies across excised human skin (Van Der Maaden et al., 2014). Vallhov *et al.* utilised a bioceramic MAP coated with OVA to deliver the antigen to dendritic cells in human skin (Vallhov et al., 2018). These studies employed different approaches to selectively quantify OVA during *in vitro* permeation studies.

Regarding *in vitro-in vivo* correlation (IVIVC), to date, such discussions have not yet been established for MAP-mediated delivery. The development of dissolving MAPs, which dissolve or degrade upon contact with skin interstitial fluid to release their drug cargo *in situ*, necessitates consideration of additional factors when designing *in vitro* permeation experiments. Ideally, the selected model membrane representing the skin barrier *in vitro* should mimic the depth of microneedle penetration, adhesion of the microneedle baseplate to the skin surface, microneedle dissolution/degradation rate (Garland et al., 2012), and subsequent drug release achieved in an *in vivo* scenario. Furthermore, given that microneedle length may exceed the thickness of the chosen skin membrane barrier, a portion of the microneedle may directly contact the receiver medium. Therefore, it is crucial to ensure that the composition of the receiver medium selected does not significantly overestimate the rate of microneedle dissolution and, consequently, the rate of drug release within the skin (Garland et al., 2012).

When observing the cumulative protein delivered from dissolving MAPs across dermatomed porcine skin in comparison to control groups, normalisation was performed by subtracting the total protein from the dissolving MAP group. Fig. 10 displays the normalised data at 24 h for OVA, BSA, and AMSC-MP released from dissolving MAPs across dermatomed porcine skin, Parafilm®M, and Strat-M®. The cumulative permeation percentages for OVA-loaded MAPs on dermatomed porcine skin, Parafilm®M, and Strat-M® were found to be 14.21%, 12.31%, and 17.27%, respectively. No significant differences were observed between the membranes after normalisation ($p > 0.05$).

For BSA, the cumulative permeation over 24 h through dermatomed porcine skin, Parafilm®M, and Strat-M® was approximately 54.45%, 26.59%, and 11.14%, respectively. Interestingly, the permeation across dermatomed porcine skin was significantly higher ($p < 0.05$) and

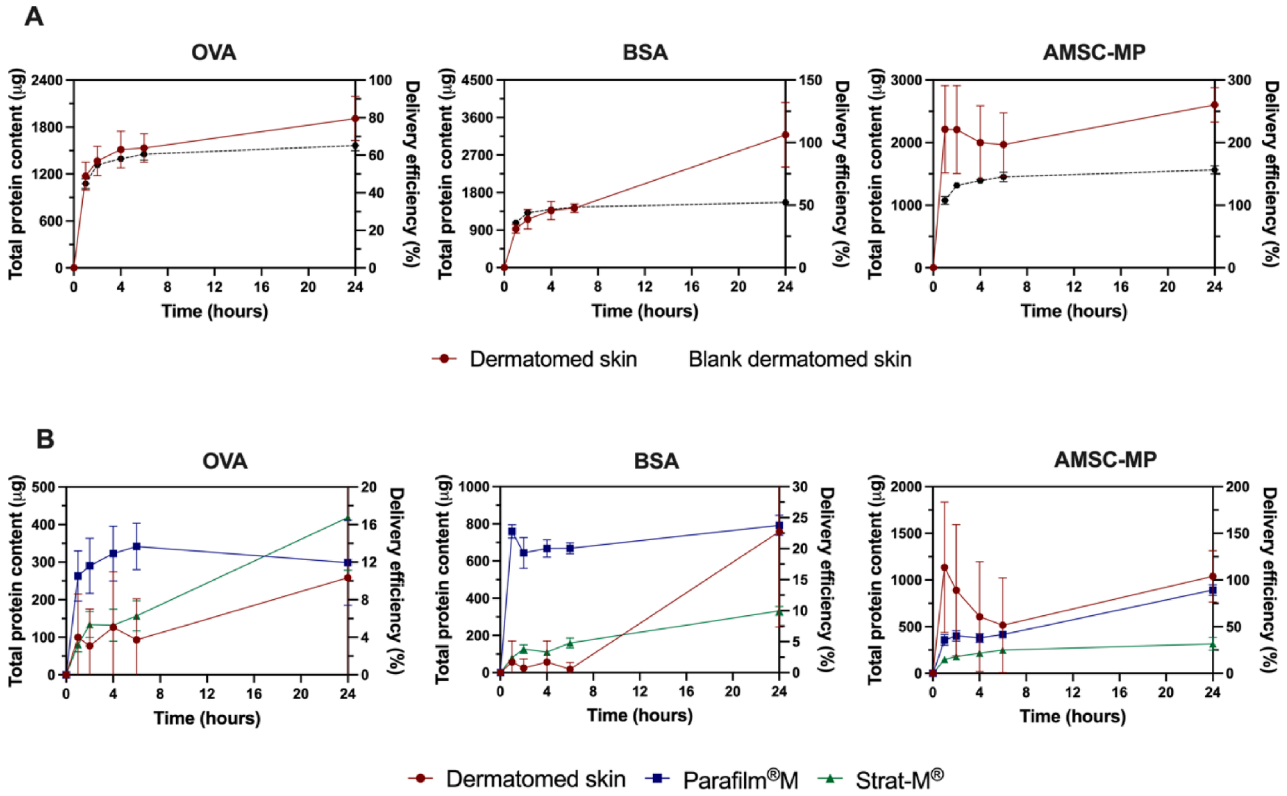

Fig. 9. (A) The total protein content was utilised to quantify the permeation of albumin derived from chicken eggs (OVA), bovine serum albumin (BSA), and amniotic mesenchymal stem cell metabolite products (AMSC-MP) from dissolving MAPs across dermatomed porcine skin. The dashed lines represent the protein released from dermatomed neonatal porcine skin without dissolving MAP application (means ± SD, n = 4). (B) The total protein content was used to quantify the permeation of albumin derived from chicken eggs (OVA), bovine serum albumin (BSA), and amniotic mesenchymal stem cell metabolite products (AMSC-MP) from dissolving MAPs across Parafilm®M, Strat-M®, and dermatomed porcine skin. Corrected values of drug permeated across dermatomed skin were obtained by subtracting the blank dermatomed skin readings (means ± SD, n = 4).

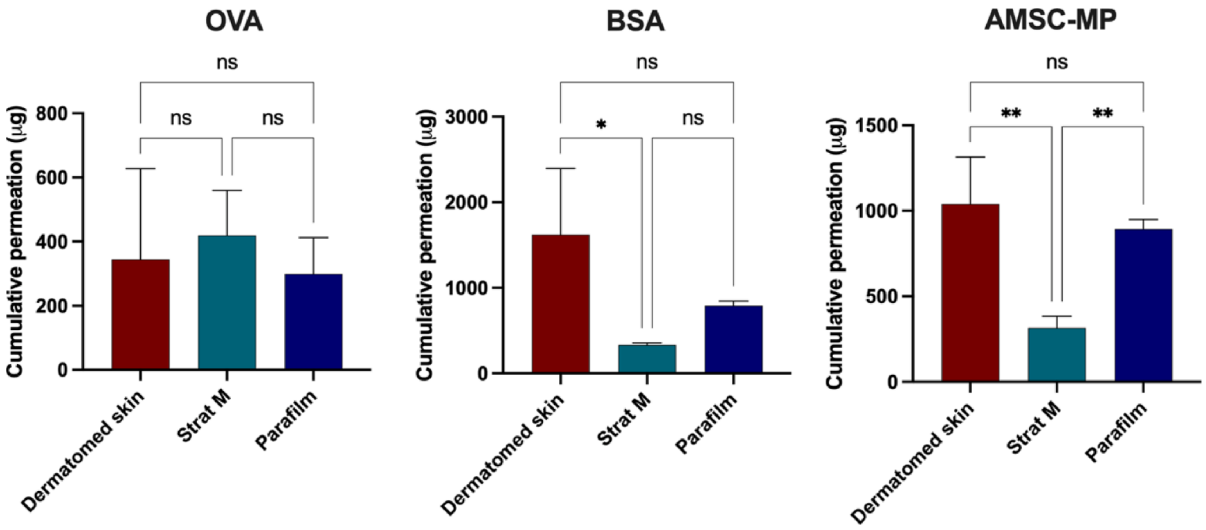

Fig. 10. Cumulative permeation of albumin derived from chicken eggs (OVA), bovine serum albumin (BSA), and amniotic mesenchymal stem cell metabolite products (AMSC-MP) across different membranes (dermatomed porcine skin, Parafilm®M and Strat-M®) over 24 h of *in vitro* permeation studies (means + SD, n = 4).

increased 4.88-fold compared to Strat-M®. This discrepancy might be attributed to skin protein presence, leading to increased protein detection across different protein models. Additionally, in AMSC-MP delivery, the cumulative permeation percentages were 110.05%, 94.59%, and 33.41% across dermatomed porcine skin, Parafilm®M, and Strat-M®, respectively. Notably, AMSC-MP permeation across Parafilm®M significantly increased by 2.83-fold compared to Strat-M® ($p < 0.05$), while there were no significant differences between Parafilm®M and dermatomed porcine skin ($p > 0.05$) in AMSC-MP permeation percentage.

The *in vitro* permeation data analysis revealed distinct correlation patterns between Parafilm®M and Strat-M® concerning the cumulative permeation of proteins within a 24-hour timeframe. These correlations appear to depend on the properties of the protein models used in the study. Fig. 11 illustrates that, based on the correlation coefficient category (Correlation and regression, n.d.); Parafilm®M exhibited strong and moderate correlations with Strat-M® for OVA and BSA, respectively. Notably, the cumulative permeation of AMSC-MP across both Parafilm®M and Strat-M® demonstrated a very strong correlation, ranging from 0.90 to 0.99.

Correlating the dermatomed porcine skin samples to both Parafilm®M and Strat-M® proved challenging due to the interference of skin proteins in the permeation results over the 24-hour period. Consequently, this study suggests that both Parafilm®M and Strat-M® outperform dermatomed neonatal porcine skin in terms of reliability in permeation studies. Furthermore, it indicates a similarity in the protein permeation profiles across Parafilm®M and Strat-M®, highlighting the potential of these skin simulants for use in protein-loaded MAPs intended for transdermal delivery. Additionally, future plans for this study include establishing a similarity factor. The current focus is on the potential use of Parafilm®M and Strat-M® in *in vitro* studies as a preliminary step to select the best formulation for *in vivo* studies using different animal models. Thus, it should also be noted that the quantified amounts using synthetic membranes might not always correlate with actual permeation studies using human or porcine skin. However, the results of this study show the potential of Parafilm®M and Strat-M® as alternatives to dermatomed porcine skin in the early-stage phase, enabling researchers to establish standardised protocols for assessing substance permeation from MAP systems.

4. Conclusion

In summary, this study demonstrates the potential use of Parafilm®M and Strat-M® as alternatives to biological skin simulants in *in vitro* permeation studies, particularly for investigating protein delivery from MAP platforms. Our findings indicate that both Parafilm® and Strat-M® exhibit only slight differences compared to dermatomed porcine skin, making them promising substitutes for membrane studies. Dermatomed porcine skin releases proteins during *in vitro* permeation studies, leading to potential interference in quantification using the BCA technique. Utilising synthetic membranes like Parafilm®M and Strat-M® can circumvent such interference, providing more reliable results compared to dermatomed neonatal porcine skin. It is important to note that while these synthetic membranes offer insights into trends and correlations, they may not precisely match absolute permeability values of biological skin membranes for protein delivery. However, these

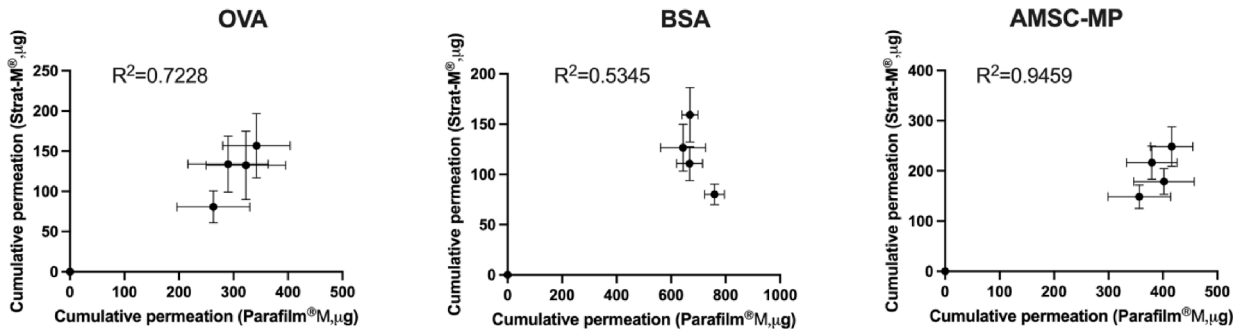

Fig. 11. Correlation of cumulative permeation between Parafilm®M and Strat-M® for albumin derived from chicken eggs (OVA), bovine serum albumin (BSA), and amniotic mesenchymal stem cell metabolite products (AMSC-MP).

results are important in understanding the potential of these membranes for formulating and optimising MAPs. These findings may serve as valuable tools for preliminary screening efforts in various MAP formulations, not limited to proteins or peptides. Synthetic membranes offer rapid, cost-effective, and easily accessible alternatives that do not require complex preparation or storage. This research marks an early-stage comparison between biological and synthetic membranes to identify a suitable skin simulant model in the field of MAP formulation.

CRediT authorship contribution statement

Qonita Kurnia Anjani: Writing – review & editing, Writing – original draft, Visualization, Validation, Methodology, Investigation, Formal analysis, Data curation, Conceptualization. **Avelia Devina Calista Nainggolan:** Investigation, Formal analysis, Data curation. **Huanhuan Li:** Investigation, Formal analysis. **Andang Miatmoko:** Writing – review & editing, Resources, Investigation. **Eneko Larrañeta:** Writing – review & editing, Visualization, Formal analysis. **Ryan F. Donnelly:** Supervision, Resources, Writing – review & editing.

Declaration of competing interest

The authors declare that they have no known competing financial interests or personal relationships that could have appeared to influence the work reported in this paper.

Data availability

Data will be made available on request.

References

Alkilani, A.Z., McCrudden, M.T.C., Donnelly, R.F., 2015. Transdermal drug delivery: innovative pharmaceutical developments based on disruption of the barrier properties of the stratum corneum. Pharmaceutics 7, 438–470. https://doi.org/10.3390/pharmaceutics7040438.

Angkawinitwong, U., Courtenay, A.J., Rodgers, A.M., Larrañeta, E., Mccarthy, H.O., Brocchini, S., Donnelly, R.F., Williams, G.R., 2020. A novel transdermal protein delivery strategy via electrohydrodynamic coating of PLGA microparticles onto microneedles. ACS Appl. Mater. Interf. 12, 12478–12488. https://doi.org/10.1021/ACSAMI.9B22425/ASSET/IMAGES/LARGE/AM9B22425_0008.JPEG.

Anjani, Q.K., Bin Sabri, A.H., Donnelly, R., 2021a. Development and validation of simple and sensitive HPLC-UV method for ethambutol hydrochloride detection following transdermal application. Anal. Methods. https://doi.org/10.1039/D1AY01414E.

Anjani, Q.K., Permana, A.D., Cárcamo-Martínez, Á., Domínguez-Robles, J., Tekko, I.A., Larrañeta, E., Vora, L.K., Ramadon, D., Donnelly, R.F., 2021b. Versatility of hydrogel-forming microneedles in in vitro transdermal delivery of tuberculosis drugs. Eur. J. Pharm. Biopharm. 294–312, 294–312. https://doi.org/10.1016/j.ejpb.2020.12.003.

Anjani, Q.K., Hidayat, A., Sabri, B., Moreno-Castellanos, N., Utomo, E., Cárcamo-Martínez, Á., Domínguez-Robles, J., Ahmadi, L., Wardoyo, H., Donnelly, R.F., 2022a. Soluplus®-based dissolving microarray patches loaded with colchicine: towards a minimally invasive treatment and management of gout. Biomater. Sci. https://doi.org/10.1039/D2BM01068B.

Anjani, Q.K., Bin Sabri, A.H., Utomo, E., Domínguez-Robles, J., Donnelly, R.F., 2022b. Elucidating the impact of surfactants on the performance of dissolving microneedle array patches. Mol. Pharm. 19, 1191–1208, 10.1021/ACS.MOLPHARMACEUT.1C00988/ASSET/IMAGES/LARGE/MP1C00988_0014.JPEG.

Anjani, Q.K., Bin Sabri, A.H., McGuckin, M.B., Li, H., Hamid, K.A., Donnelly, R.F., 2022c. In vitro permeation studies on carvedilol containing dissolving microarray patches quantified using a rapid and simple HPLC-UV analytical method. AAPS PharmSciTech 23, 1–13. https://doi.org/10.1208/S12249-022-02422-6/FIGURES/4.

Anjani, Q.K., Bin Sabri, A.H., Domínguez-Robles, J., Moreno-Castellanos, N., Utomo, E., Wardoyo, L.A.H., Larrañeta, E., Donnelly, R.F., 2022d. Metronidazole nanosuspension loaded dissolving microarray patches: An engineered composite pharmaceutical system for the treatment of skin and soft tissue infection. Biomaterials Adv. 140, 213073 https://doi.org/10.1016/J.BIOADV.2022.213073.

Anjani, Q.K., Bin Sabri, A.H., Hutton, A.J., Cárcamo-Martínez, Á., Wardoyo, L.A.H., Mansoor, A.Z., Donnelly, R.F., 2023a. Microarray patches for managing infections at a global scale. J. Control. Release 359, 97–115. https://doi.org/10.1016/j.jconrel.2023.05.038.

Anjani, Q.K., Bin Sabri, A.H., Hamid, K.A., Moreno-Castellanos, N., Li, H., Donnelly, R.F., 2023b. Tip loaded cyclodextrin-carvedilol complexes microarray patches. Carbohydr. Polym. 320, 121194 https://doi.org/10.1016/j.carbpol.2023.121194.

Anjani, Q.K., Pandya, A.K., Demartis, S., Domínguez-Robles, J., Moreno-Castellanos, N., Li, H., Gavini, E., Patravale, V.B., Donnelly, R.F., 2023c. Liposome-loaded polymeric microneedles for enhanced skin deposition of rifampicin. Int. J. Pharm. 646, 123446 https://doi.org/10.1016/J.IJPHARM.2023.123446.

Anjani, Q.K., Cárcamo-Martínez, Á., Wardoyo, L.A.H., Moreno-Castellanos, N., Bin Sabri, A.H., Larrañeta, E., Donnelly, R.F., 2023d. MAP-box: a novel, low-cost and easy-to-fabricate 3D-printed box for the storage and transportation of dissolving microneedle array patches. Drug Deliv. Transl. Res. https://doi.org/10.1007/s13346-023-01393-w.

Anjani, Q.K., Bin Sabri, A.H., Hamid, K.A., Moreno-Castellanos, N., Li, H., Donnelly, R.F., 2023e. Tip loaded cyclodextrin-carvedilol complexes microarray patches. Carbohydr. Polym. 320, 121194.

Anjani, Q.K., Volpe-Zanutto, F., Hamid, K.A., Bin Sabri, A.H., Moreno-Castellano, N., Gaitán, X.A., Calit, J., Bargieri, D.Y., Donnelly, R.F., 2023f. Primaquine and chloroquine nano-sized solid dispersion-loaded dissolving microarray patches for the improved treatment of malaria caused by Plasmodium vivax. J. Controll. Release 361, 385–401. https://doi.org/10.1016/J.JCONREL.2023.08.009.

Antosova, Z., Mackova, M., Kral, V., Macek, T., 2009. Therapeutic application of peptides and proteins: parenteral forever? Trends Biotechnol. 27, 628–635. https://doi.org/10.1016/J.TIBTECH.2009.07.009.

Badhe, R.V., Adkine, D., Godse, A., 2021. Development of polylactic acid and bovine serum albumin-layered-coated chitosan microneedles using novel bees wax mould. Turk. J. Pharm. Sci. 18, 367. https://doi.org/10.4274/TJPS.GALENOS.2020.47897.

Bin Sabri, A.H., Anjani, Q.K., Donnelly, R.F., Hidayat Bin Sabri, A., Kurnia Anjani, Q., Donnelly, R.F., 2021. Synthesis and characterization of sorbitol laced hydrogel-forming microneedles for therapeutic drug monitoring. Int. J. Pharm. 607, 121049.

Bin Sabri, A.H., Anjani, Q.K., Utomo, E., Ripolin, A., Donnelly, R.F., 2022. Development and characterization of a dry reservoir-hydrogel-forming microneedles composite for minimally invasive delivery of cefazolin. Int. J. Pharm. 617, 121593 https://doi.org/10.1016/J.IJPHARM.2022.121593.

Bittner, B., Richter, W., Schmidt, J., 2018. Subcutaneous administration of biotherapeutics: an overview of current challenges and opportunities. BioDrugs 32, 425. https://doi.org/10.1007/S40259-018-0295-0.

Bruno, B.J., Miller, G.D., Lim, C.S., 2013. Basics and recent advances in peptide and protein drug delivery. Ther. Deliv. 4, 1443. https://doi.org/10.4155/TDE.13.104.

Caudill, C.L., Perry, J.L., Tian, S., Luft, J.C., DeSimone, J.M., 2018. Spatially controlled coating of continuous liquid interface production microneedles for transdermal protein delivery. J. Control. Release 284, 122–132. https://doi.org/10.1016/J.JCONREL.2018.05.042.

Cordeiro, A.S., Tekko, I.A., Jomaa, M.H., Vora, L., McAlister, E., Volpe-Zanutto, F., Nethery, M., Baine, P.T., Mitchell, N., McNeill, D.W., Donnelly, R.F., 2020. Two-photon polymerisation 3D printing of microneedle array templates with versatile designs: application in the development of polymeric drug delivery systems. Pharm. Res. 37, 1–15. https://doi.org/10.1007/S11095-020-02887-9/FIGURES/9.

11. Correlation and regression, (n.d.). https://www.bmj.com/about-bmj/resources-readers/publications/statistics-square-one/11-correlation-and-regression (Accessed December 2, 2023).

Demir, Y.K., Akan, Z., Kerimoglu, O., 2013. Sodium alginate microneedle arrays mediate the transdermal delivery of bovine serum albumin. PLoS One 8, e63819.

Donnelly, R.F., Prausnitz, M.R., 2023. The promise of microneedle technologies for drug delivery. Drug Deliv. Transl. Res. 1–8. https://doi.org/10.1007/S13346-023-01430-8/FIGURES/2.

Donnelly, R.F., Garland, M.J., Morrow, D.I.J., Migalska, K., Singh, T.R.R., Majithiya, R., Woolfson, A.D., 2010. Optical coherence tomography is a valuable tool in the study of the effects of microneedle geometry on skin penetration characteristics and in-skin dissolution. J. Control. Release 147, 333–341. https://doi.org/10.1016/J.JCONREL.2010.08.008.

Donnelly, R.F., Majithiya, R., Singh, T.R.R., Morrow, D.I.J., Garland, M.J., Demir, Y.K., Migalska, K., Ryan, E., Gillen, D., Scott, C.J., Woolfson, A.D., 2011. Design, optimization and characterisation of polymeric microneedle arrays prepared by a novel laser-based micromoulding technique. Pharm. Res. 28, 41–57. https://doi.org/10.1007/S11095-010-0169-8/FIGURES/12.

Doughty, D.V., Clawson, C.Z., Lambert, W., Subramony, J.A., 2016. Understanding subcutaneous tissue pressure for engineering injection devices for large-volume protein delivery. J. Pharm. Sci. 105, 2105–2113. https://doi.org/10.1016/J.XPHS.2016.04.009.

Garland, M.J., Migalska, K., Tuan-Mahmood, T.M., Raghu Raj Singh, T., Majithija, R., Caffarel-Salvador, E., McCrudden, C.M., McCarthy, H.O., David Woolfson, A., Donnelly, R.F., 2012. Influence of skin model on in vitro performance of drug-loaded soluble microneedle arrays. Int. J. Pharm. 434, 80–89. https://doi.org/10.1016/J.IJPHARM.2012.05.069.

Haq, A., Goodyear, B., Ameen, D., Joshi, V., Michniak-Kohn, B., 2018. Strat-M® synthetic membrane: permeability comparison to human cadaver skin. Int. J. Pharm. 547, 432–437. https://doi.org/10.1016/J.IJPHARM.2018.06.012.

Jiskoot, W., Randolph, T.W., Volkin, D.B., Middaugh, C.R., Schöneich, C., Winter, G., Friess, W., Crommelin, D.J.A., Carpenter, J.F., 2012. Protein instability and immunogenicity: roadblocks to clinical application of injectable protein delivery systems for sustained release. J. Pharm. Sci. 101, 946–954. https://doi.org/10.1002/JPS.23018.

Kirkby, M., Hutton, A.R.J., Donnelly, R.F., 2020. Microneedle mediated transdermal delivery of protein, peptide and antibody based therapeutics: current status and future considerations. Pharm. Res. 37, 1–18. https://doi.org/10.1007/S11095-020-02844-6/TABLES/2.

E. Larrañeta, M.T.C. McCrudden, A.J. Courtenay, R.F. Donnelly, Microneedles: a new frontier in nanomedicine delivery, Pharmaceut. Res. 33 (2016) 1055–1073. doi: 10.1007/S11095-016-1885-5.

Larrañeta, E., Moore, J., Vicente-Pérez, E.M., González-Vázquez, P., Lutton, R., Woolfson, A.D., Donnelly, R.F., 2014. A proposed model membrane and test method for microneedle insertion studies. Int. J. Pharm. 472, 65–73. https://doi.org/10.1016/j.ijpharm.2014.05.042.

Larrañeta, E., Stewart, S., Fallows, S.J., Birkhäuer, L.L., McCrudden, M.T.C., Woolfson, A. D., Donnelly, R.F., 2016. A facile system to evaluate in vitro drug release from dissolving microneedle arrays. Int. J. Pharm. 497, 62–69. https://doi.org/10.1016/J.IJPHARM.2015.11.038.

R. Neupane, S.H.S. Boddu, J. Renukuntla, R.J. Babu, A.K. Tiwari, Alternatives to biological skin in permeation studies: current trends and possibilities, Pharmaceutics 12 (2020) 152. doi: 10.3390/PHARMACEUTICS12020152.

Oberli, M.A., Schoellhammer, C.M., Langer, R., Blankschtein, D., 2014. Ultrasound-enhanced transdermal delivery: recent advances and future challenges. Ther. Deliv. 5, 843–857. https://doi.org/10.4155/tde.14.32.

Pulsoni, I., Lubda, M., Aiello, M., Fedi, A., Marzagalli, M., von Hagen, J., Scaglione, S., 2022. Comparison between franz diffusion cell and a novel micro-physiological system for in vitro penetration assay using different skin models. SLAS Technol. 27, 161–171. https://doi.org/10.1016/J.SLAST.2021.12.006.

Uchida, T., Nishioka, K., Motoki, A., Yakumaru, M., Sano, T., Todo, H., Sugibayashi, K., 2016. Effect of esters on the permeation of chemicals with different polarities through synthetic artificial membranes using a high-throughput diffusion cell array. Chem. Pharm. Bull. (Tokyo) 64, 1597–1606. https://doi.org/10.1248/CPB.C16-00480.

Vallhov, H., Xia, W., Engqvist, H., Scheynius, A., 2018. Bioceramic microneedle arrays are able to deliver OVA to dendritic cells in human skin. J. Mater. Chem. B 6, 6808–6816. https://doi.org/10.1039/C8TB01476K.

Van Der Maaden, K., Varypataki, E.M., Romeijn, S., Ossendorp, F., Jiskoot, W., Bouwstra, J., 2014. Ovalbumin-coated pH-sensitive microneedle arrays effectively induce ovalbumin-specific antibody and T-cell responses in mice. Eur. J. Pharm. Biopharm. 88, 310–315. https://doi.org/10.1016/J.EJPB.2014.05.003.

Vora, L.K., Sabri, A.H., Naser, Y., Himawan, A., Hutton, A.R.J., Anjani, Q.K., Volpe-Zanutto, F., Mishra, D., Li, M., Rodgers, A.M., Paredes, A.J., Larrañeta, E., Thakur, R. R.S., Donnelly, R.F., 2023. Long-acting microneedle formulations. Adv. Drug Deliv. Rev. 201, 115055 https://doi.org/10.1016/J.ADDR.2023.115055.